

Study of the phase transition in lithium ammonium tartrate monohydrate (LAT) by means of infrared and Raman spectroscopy

This article has been downloaded from IOPscience. Please scroll down to see the full text article.

1996 J. Phys.: Condens. Matter 8 8669

(<http://iopscience.iop.org/0953-8984/8/44/016>)

View [the table of contents for this issue](#), or go to the [journal homepage](#) for more

Download details:

IP Address: 171.66.16.207

The article was downloaded on 14/05/2010 at 04:26

Please note that [terms and conditions apply](#).

Study of the phase transition in lithium ammonium tartrate monohydrate (LAT) by means of infrared and Raman spectroscopy

S Kamba^{†‡}, B Březina[†], J Petzelt[†] and G Schaack[‡]

[†] Institute of Physics, Academy of Sciences of the Czech Republic, Na Slovance 2,
180 40 Prague 8, Czech Republic

[‡] Physikalisches Institut der Universität Würzburg, Am Hubland, D-97074 Würzburg, Germany

Received 12 June 1996

Abstract. Infrared and Raman spectra of lithium ammonium tartrate monohydrate were obtained in the frequency region $10\text{--}700\text{ cm}^{-1}$ at temperatures of $15\text{--}300\text{ K}$. No soft phonon mode was observed, so the ferroelastic and ferroelectric phase transition at $T_c = 98\text{ K}$ is of order–disorder type. The ordering of atoms below T_c produces pronounced decreases in the dampings of all phonon modes. The change in the number of infrared and Raman-active modes at the phase transition seems to correspond to the transition from the orthorhombic to a monoclinic phase instead of the recently predicted triclinic low-temperature phase. In contrast to the case for isomorphous lithium thallium tartrate monohydrate, where a substantial increase of T_c with hydrostatic pressure was observed, in the case of LAT crystal T_c decreases only slightly down to 91 K at 400 MPa .

1. Introduction

A ferroelectric phase transition (PT) in lithium ammonium tartrate monohydrate (LAT)— $\text{LiNH}_4\text{C}_4\text{H}_4\text{O}_6\cdot\text{H}_2\text{O}$ —was discovered by Matthias and Hulm [1] and independently by Merz [2] in 1951. The second-order PT from a paraelectric (PE) orthorhombic phase (space group $P2_12_12$ (D_2^3), $Z = 4$) [3, 4] to a ferroelectric (FE) monoclinic phase (space group $P12_11$, $Z = 4$) [3] occurs at $T_c = 98\text{ K}$.

The crystal structure of LAT is in the PE phase isomorphous with lithium thallium tartrate monohydrate (LTT) and with lithium rubidium tartrate monohydrate (LRT). However, in the FE phase the spontaneous polarization P_s of LAT appears parallel to the crystallographic b -axis, while P_s for LTT is parallel to the a -axis and LRT exhibits no FE PT. This fact indicates the important role of the NH_4 ions for the occurrence of the FE state in LAT. X-ray refinement [4] of the LAT crystal structure in the PE phase revealed two sets of inequivalent positions of NH_4 ions on the twofold-symmetry axes. The distribution of the hydrogen atoms around the central N atom is different in the two sets. One set of NH_4 ions exhibits a large thermal motion of the hydrogen atoms, which suggests the possibility of disorder in the orientation of these NH_4 ions [4]. However, Abe and Matsuda have shown that it is not the NH_4 ion, but one from the hydroxyl groups of the tartrate molecule that is responsible for a ferroelectric dipole in LAT [5]. The same hydroxyl group is also responsible for the FE properties of Rochelle salt (sodium potassium tartrate tetrahydrate), where the configuration of atoms in the tartrate molecule resembles that of LAT [6, 7].

Maeda *et al* [8, 9] performed an ESR experiment on LAT and found that P_s can be reversed not only by applying an electric field but also by applying a shear stress σ_{ca} . This indicates that LAT is both ferroelectric and ferroelastic below T_c . Other dielectric and Brillouin scattering measurements [10, 11] revealed that the primary order parameter of the PT is the shear strain x_5 (a direct observation of its temperature dependence is published in reference [12]), which gives rise to ferroelectricity through the piezoelectric coupling with the polarization [10].

However, the single order parameter of B_2 symmetry cannot explain the observed small anomalies in the dielectric constant $\epsilon'_a(T)$ [13] and in the elastic compliance s_{44}^E near T_c [13]. These effects can be understood if the FE phase does not have the monoclinic structure considered earlier but has the triclinic one. Indications of the triclinic symmetry in the FE phase were observed in EPR studies [14] and also in a recent careful dielectric measurement [15]. In this case a two-component order parameter (OP) from the Brillouin zone (BZ) boundary was suggested [15].

In this paper we present the results of our infrared, far-infrared and Raman spectroscopic measurements from which we derive the order-disorder type of the PT (lack of the soft phonon mode). Our results do not support the triclinic symmetry of the FE phase claimed recently [14, 15] but are fully consistent with the monoclinic $P2_1$ structure. In addition, high-pressure dielectric measurements were performed showing a surprisingly small effect on the PT temperature.

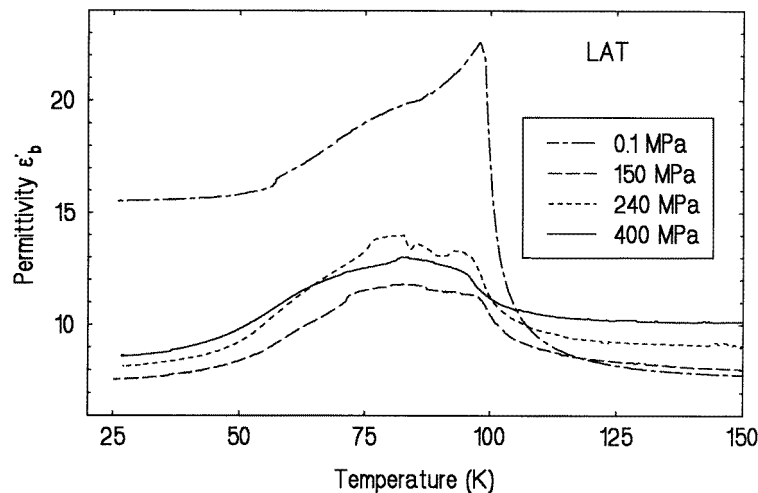


Figure 1. Temperature dependences of the permittivity ϵ'_b at ambient and elevated hydrostatic pressures. All of the curves were obtained on cooling and at 10 kHz.

2. Experimental details

Colourless LAT single crystals of good optical quality with volumes of several cm^3 were grown from aqueous solution. For the infrared (IR) and dielectric measurements, plate-like samples (diameter 5–10 mm, thickness 0.18–2 mm) were cut from the single crystal. The sample for Raman scattering had a rectangular shape ($\sim 4 \times 3 \times 6 \text{ mm}^3$) with the edges parallel to the crystallographic axes. All of the samples were oriented in polarized light and optically

polished. The permittivity ϵ'_b and dielectric loss ϵ''_b were measured in the temperature region 20–300 K at ambient and also at hydrostatic pressures up to 400 MPa using Wayne–Kerr automatic bridge operating at frequencies of $f = 0.1, 0.4, 1, 10$ kHz. Helium gas was used as a pressure medium. The measuring field was 3 V cm^{-1} . The temperature drift with the rate of $5 \text{ K h}^{-1} \leq |dT/dt| \leq 15 \text{ K h}^{-1}$ was controlled automatically.

Polarized IR reflectivity and transmission spectra in the range $10\text{--}650 \text{ cm}^{-1}$ were obtained using a Grubb–Parsons Fourier spectrometer equipped with a helium-cooled Si bolometer. Resolutions of 2 cm^{-1} in the reflectivity spectra and 1 cm^{-1} in the transmission spectra were achieved.

The Raman scattering spectra were obtained using a Dilor XY spectrometer equipped with a liquid-nitrogen-cooled CCD detector. An argon laser with $\lambda = 514.5 \text{ nm}$ was used as the excitation source with the power of the beam impinging on the sample being 100–200 mW to protect the sample against heating. All of the spectra were taken in 90° scattering geometry in the range $5\text{--}700 \text{ cm}^{-1}$ at temperatures of 15–300 K with the spectral resolution of 2.5 cm^{-1} .

3. Experimental results

3.1. The high-pressure dielectric measurement

The permittivity and dielectric loss were measured using a plate-shaped sample 0.56 mm thick with the orientation (010). The temperature dependence of the permittivity ϵ'_b at several hydrostatic pressures up to 400 MPa is depicted in figure 1. Our sample was partially mechanically clamped; therefore the anomaly in ϵ'_b near T_c is relatively small in comparison with the result in reference [2]. The PT in LAT is a proper ferroelastic one; therefore the anomaly ϵ'_b in the clamped crystal should disappear [10]. Like in other ferroelectrics with hydrogen bonds (KDP family [16], LTT [17]), the permittivity ϵ'_b does not decrease quickly below T_c and a broad maximum appears as a consequence of the domain wall contribution. As usual [18], the anomaly in ϵ'_b decreases with increasing hydrostatic pressure. All of the ϵ'_b -curves were fitted above T_c with the Curie–Weiss formula. In contrast with the case for isomorphous LTT crystal, where a substantial increase of the FE PT temperature with increasing pressure was recently observed [17], in the case of LAT T_c decreases slowly from 98 K at ambient pressure down to 91 K at 400 MPa.

3.2. The infrared and Raman experiment

The results of polarized IR reflectivity measurements at various temperatures are seen in figures 2(a)–2(c). A sample 1 mm thick was used in the case of the polarization with $\mathbf{E} \parallel \mathbf{b}$; therefore a high reflectivity increase appears at low frequencies below 60 cm^{-1} and at low temperatures owing to partial transparency and multiple reflection (figure 2(b)). A sample more than two times thicker was used in the rest of the measurements (figures 2(a) and 2(c)) to eliminate this effect.

FIR transmission spectra are presented only in the region below 110 cm^{-1} ; at higher frequencies the samples (thickness $170\text{--}200 \mu\text{m}$) were almost opaque. The example of FIR transmission spectra for the polarization with $\mathbf{E} \parallel \mathbf{b}$ (FE axis) is depicted in figure 3. The transmission is rather high; therefore besides phonon absorption bands at $\sim 55, 67, 76$ and 90 cm^{-1} also interference from the plane-parallel sample surfaces appears in the spectra. The damping of all of the modes decreases substantially below the PT temperature, and therefore the absolute value of the transmissivity and reflectivity increases on cooling and

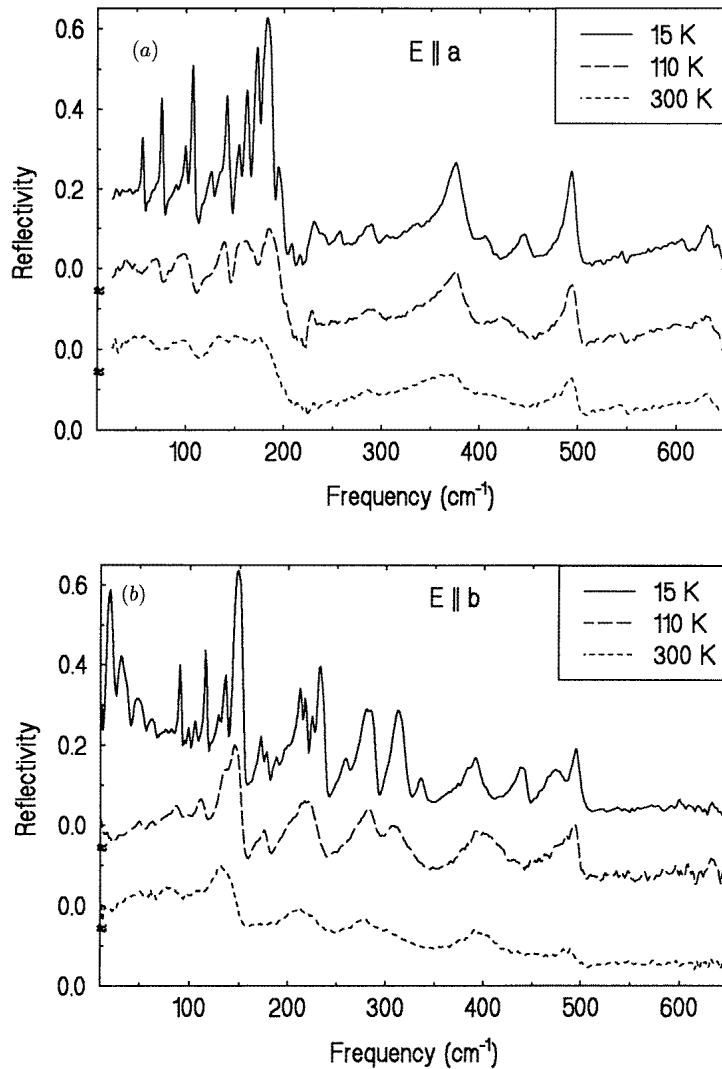


Figure 2. Infrared reflectivity spectra of LAT single crystal for the polarization with (a) $E \parallel a$, (b) $E \parallel b$ and (c) $E \parallel c$. Note that $T_c = 98$ K. The structures in figure 2(b) below 60 cm^{-1} are artefacts due to the high transparency of the sample (1 mm thick). The minima are due to absorption lines.

a rich fine structure in the spectra appears. The same—but even more pronounced—effect is seen in the Raman spectra (figure 4).

All of the IR spectra were fitted with the model of the sum of classical harmonic oscillators. Lists of all of the phonon frequencies obtained from Raman and IR spectra at 110 K (PE phase) and at 15 K (FE phase) are presented in tables 1 and 2, respectively. The increase in the number of observed modes in the FE phase is evident. However, not all of the new modes indicated in the FE phase are really new—they were just not resolved in the spectra of the PE phase as a consequence of the substantial damping of all of the modes.

In contrast to the case for the previously studied materials Rochelle salt [19], and LTT

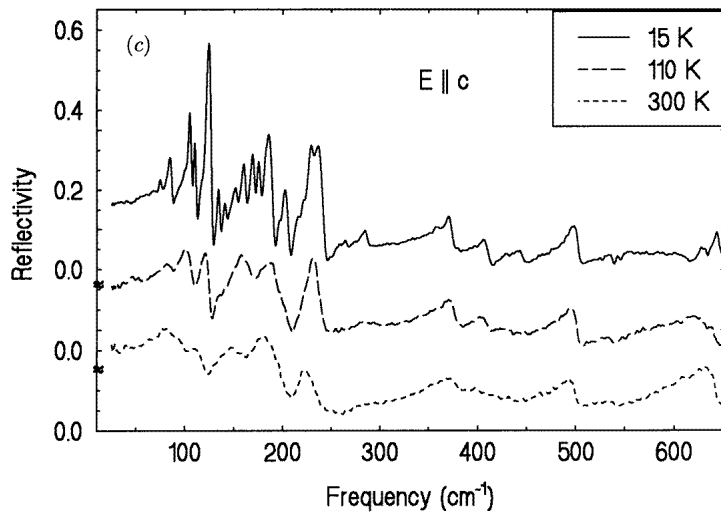
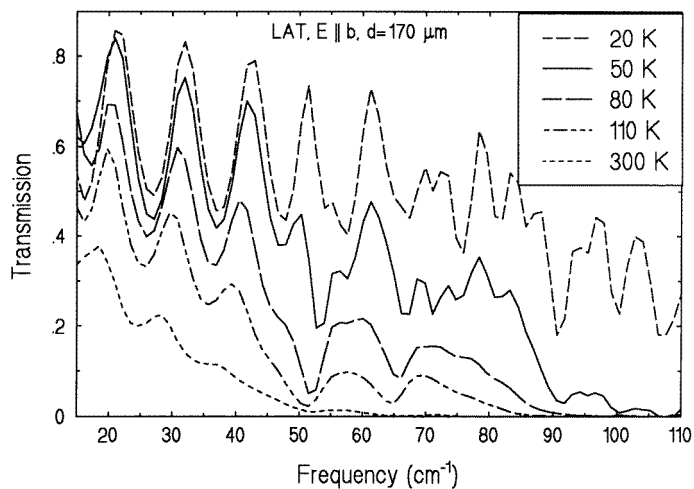


Figure 2. (Continued)

Figure 3. FIR transmission spectra for $E \parallel b$ at several temperatures in the paraelectric and the ferroelectric phase.

[17] no optic soft mode was observed in LAT. This to be expected for LAT as an improper FE with the shear strain as the primary order parameter of the PT.

4. Discussion

How many vibrational modes can we expect theoretically in our spectra? In the PE phase, the unit cell contains four formula units; therefore 276 vibrational modes are expected in total. Except the N atoms which have C_2 site symmetry, all of the atoms occupy general positions (C_1 site symmetry) of the lattice. Therefore the lattice vibrations at the Γ point of

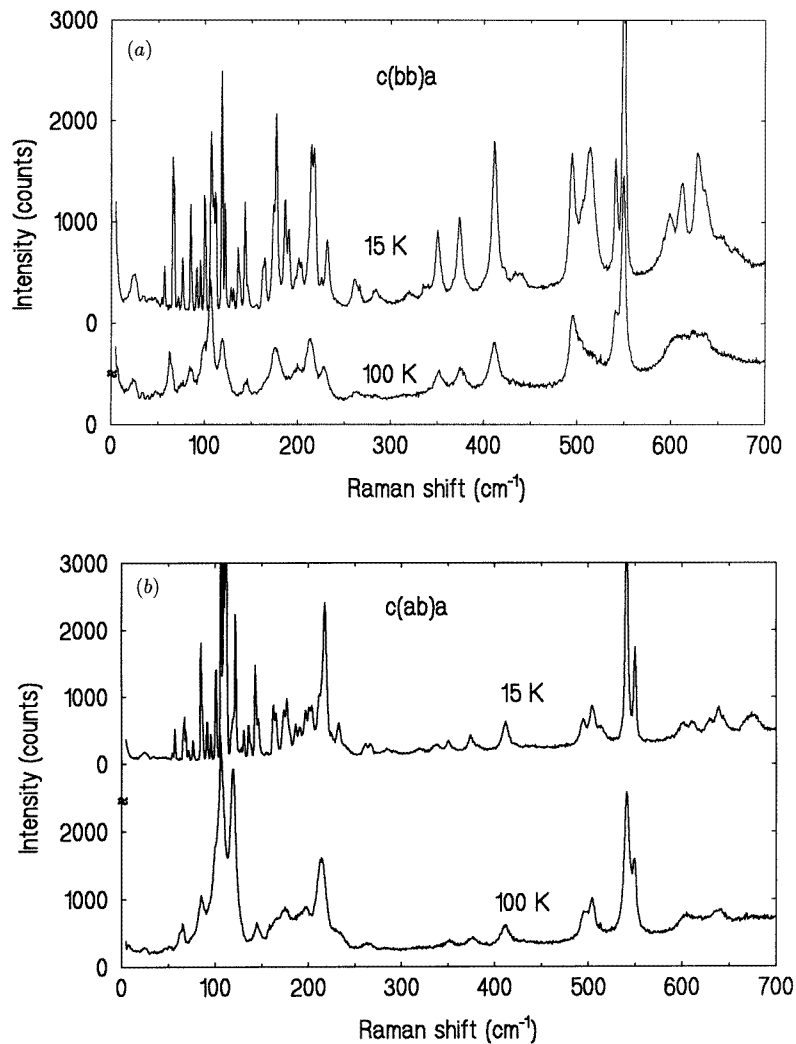


Figure 4. Raman spectra of (a) *bb*, (b) *ab*, (c) *ac* and (d) *bc* symmetries in the paraelectric (100 K) and the ferroelectric phase (15 K). All of the spectra were accumulated for 200 s.

the Brillouin zone have in the PE phase ($P2_12_12$) the following symmetries and activities in the spectra:

$$\Gamma_{\text{PE}} = 68A(a^2, b^2, c^2) + 67B_1(c, ab) \\ + 69B_2(b, ac) + 69B_3(a, bc) + (B_1 + B_2 + B_3)_{\text{acoustic}}$$

The letters in brackets specify the elements of the Raman tensor and the polarization of the IR radiation parallel to the orthorhombic lattice vectors. This means that the A modes are only Raman active, while the B_1 , B_2 and B_3 modes are active both in Raman and in IR spectra.

Considering the tartrate, ammonium and water molecules as rigid units, we can specify

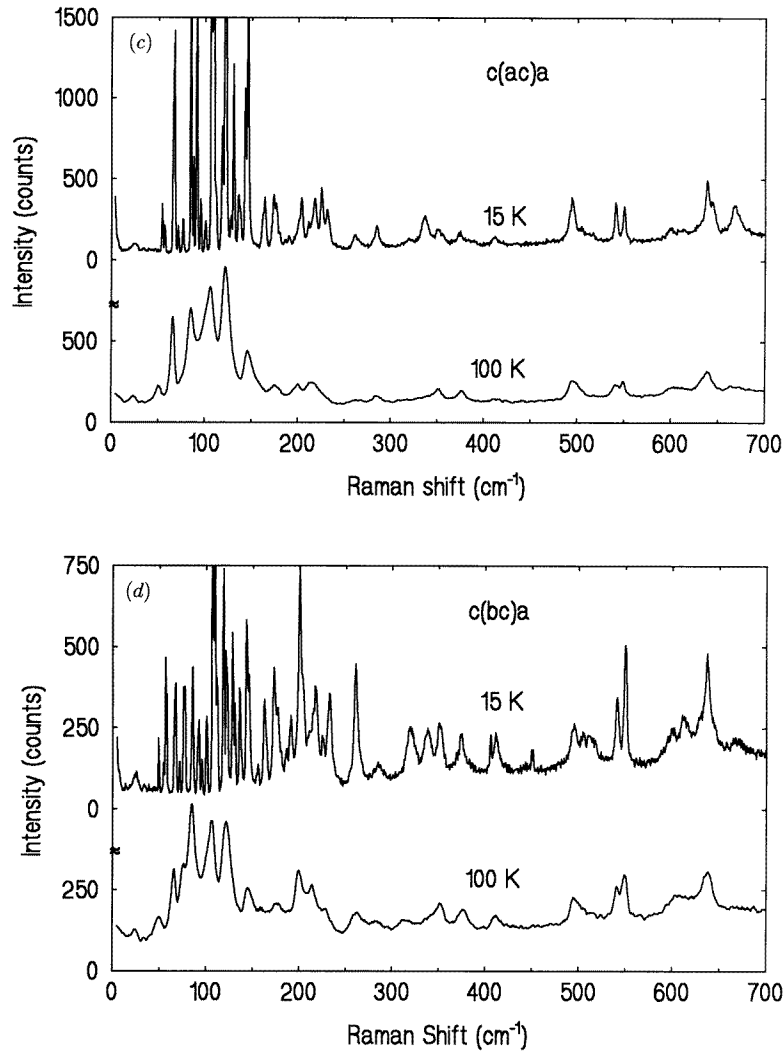


Figure 4. (Continued)

the low-frequency external modes (without acoustic modes):

$$\Gamma_{\text{PE external}} = 19A + 18B_1 + 22B_2 + 22B_3.$$

These modes mostly have lower frequencies than the internal vibrations of tartrate, ammonium and water groups, and lie typically below 300 cm⁻¹.

If the LAT crystal undergoes an equitranslational PT to the FE phase with the monoclinic space group *P12₁1* as was proposed in [3, 4], the IR and Raman activities of all of the modes from the Brillouin zone centre should be as follows:

$$\Gamma_{\text{FE}} = 137A(b, ac, a^2, b^2, c^2) + 136B(a, c, ab, bc) + (A + 2B)_{\text{acoustic}}.$$

The external modes of these are

$$\Gamma_{\text{FE external}} = 41A + 40B.$$

Table 1. The frequencies of the Raman-active modes in the PE phase (110 K) and in the FE phase (15 K). A, B, B₁, B₂ and B₃ specify the symmetries of phonon modes. All of the frequencies are in cm⁻¹.

A(bb) 110 K	A(bb) 15 K	B ₂ (ac) 110 K	A(ac) 15 K	B ₁ (ab) 110 K	B(ab) 15 K	B ₃ (bc) 110 K	B(bc) 15 K
25.0	25.0			~ 25.0	~ 25.0	~ 25.0	~ 25.0
	56.9	51.5	53.9		56.7	50.4	49.4
63.0	66.3	65.7	66.3	65.7	66.3	65.7	66.3
	71.2		71.2		71.2		71.2
	76.3		76.3		76.3	75.0	76.3
84.7	84.6	84.7	84.6	84.7	84.6	84.7	84.6
	91.1		90.8		91.1		
	95.0	92.7	95.0		95.0		
	100.0		100.0		100.5		100.0
105.5	106.5	105.5	106.5	105.5	106.4	105.5	106.4
	109.0		109.0		109.0		109.0
	111.4		111.4		111.4		111.4
118.6	118.3		118.3	118.6	118.3		118.3
	121.7	121.3	121.7		121.7	121.3	121.7
	128.0						128.0
	130.5		130.5		130.5		130.5
	135.7		135.7		135.7		135.7
	142.8		142.8	145.0	142.8	145.0	142.8
	145.7	146.3	145.7		142.8		
	162.1		162.1	164.3	162.1		162.1
	173.5		173.5		173.5		173.5
175.0	176.5		176.5	175.0	176.5		176.5
	186.0				186.0		
	190.0				190.4		190.4
195.7	200.7		200.7		200.2	199.3	200.2
	203.4		203.4		203.4		203.4
213.2	214.3			213.2	211.4		
	217.4		217.4		217.4		217.4
227.2	231.1		231.1		232.1		232.1
	260.5		261.0		261.0		260.5
	283.5		284.4		266.7		
			336.0				338.0
352.5	350.3			352.5	350.3	352.5	350.3
375.3	373.5			375.3	373.5	375.3	373.5
411.1	411.3			411.1	411.3	411.1	411.3
495.6	494.4	495.6	494.3	495.6	494.3		
	513.4				503.7		504.1
540.8	541.0	540.8	541.0	540.8	541.0	540.8	541.0
549.0	550.0	549.0	550.0	549.0	550.0	549.0	550.0
~ 606.0	611.3			~ 606.0	611.3		
637.7	637.3	637.7	638.0	637.7	638.0	637.7	637.3

If a doubling of the unit cell occurred below T_c and the low-temperature phase had triclinic symmetry, as was recently suggested by Glushkov *et al* [15], then all of the 552 vibrational modes would be of A symmetry. In this case we could see in the FE phase each vibrational mode in all types of IR and Raman spectra, however with widely different intensities. This means that the number of modes to be seen in each spectrum should be up to eight times higher below T_c than in the PE phase. Lists of all of the phonon frequencies

Table 2. Frequencies of the IR-active modes; compare table 1. δ , β and τ represent the angle of deformation, bond bending and torsion, respectively, of the groups indicated. All frequencies are in cm^{-1} .

$E\parallel a$		$E\parallel b$		$E\parallel c$		Assignment
$B_3(a)$	$B(a)$	$B_2(b)$	$A(b)$	$B_3(c)$	$B(c)$	
110 K	15 K	110 K	15 K	110 K	15 K	
			25.5			Libration of tartrate
			40.7			
51.0	56.2	51.0	56.5			}
		64.5	67.0			
71.8	75.5		75.6		75.8	}
				84.4	85.4	
	91.3	89.2	91.0		93.5	}
99.7	100.6	99.1	100.1		100.6	
	106.6		106.3	102.6	105.2	$\beta_{C(OH)}$
		113.7	116.4		109.9	
121.4	126.1		129.7	120.9	122.9	δ_{CCC}
131.3	135.5	136.4	136.3	135.3	134.1	
				141.3	141.3	CC twist and external lattice modes
		144.9	146.4		147.4	
154.4	154.4			150.3	151.9	}
				157.5	159.8	
161.1	161.7	168.5	173.0	164.5	168.8	}
167.5	171.2	176.9	178.6	177.3	175.1	
181.6	179.0		189.0	186.6	183.5	}
	193.4		200.6	197.5	195.9	
202.3	207.7	205.3	212.5	202.3	201.7	}
		215.6	217.6		215.4	
		222.5	224.4	219.6	220.9	}
	232.0	230.2	231.2	229.7	227.4	
	240.2			237.9	233.7	δ_{CCC}
	257.3	251.6	259.8		258.3	
					264.1	$\delta_{C(OH)}$
			279.4		273.4	
296.1	289.2	283.5	285.0	291.0	283.2	}
	306.8	309.2	311.0	327.0	359.0	
340.7	338.3	328.3	335.5	355.4	359.0	}
374.0	371.4		391.1	370.8	369.3	
	404.2	399.5	404.6	404.6	406.4	$\beta_{C(OH)}$
426.0	444.8	435.1	439.7	429.0	441.2	
491.7	490.0	481.1	474.4	495.2	496.9	δ_{COO}
606.6	606.5			600.5	631.4	
632.7	631.2			624.3	631.4	τ_{COO}

obtained from all of the Raman and IR spectra in the PE (110 K) and FE (15 K) phases are presented in tables 1 and 2. In fact, we see many vibrational modes active in more spectra simultaneously (especially in the Raman spectra). However, this is the case also in the PE phase where they should have different symmetry. It is possible that different vibrations exist with similar or even the same frequencies; however, a second reason is more probable: the laser beam in the Raman experiment is not ideally polarized along the crystallographic axes due to crystal imperfections which produces a leakage of the modes into otherwise forbidden spectra.

For example the mode at 25 cm^{-1} , which is strongly active in the bb spectra, is only

weak in other Raman spectra. The A symmetry of this mode is supported by its IR activity in the $\mathbf{E}\parallel\mathbf{b}$ spectrum at 15 K. This mode is very weak in the IR spectra, and therefore it is not seen in our FIR transmission spectra for the thin sample (figure 3), but only in the low-temperature reflection spectra (figure 2(b)), where the sample that is 1 mm thick is so highly transparent below 60 cm^{-1} that the reflection from the back surface of the sample contributes to the observed reflection at low temperatures and the minima in the spectra at 25.5 , 40.7 and 56.5 cm^{-1} correspond to weak absorption peaks. The mode at 25 cm^{-1} is practically temperature independent and is assigned mainly to the tartrate libration. A mode of similar frequency was observed also in the isomorphous LTT crystal and in the chemically similar Rochelle salt [17, 19]. Most remarkably, this latter mode is the soft mode in these compounds which drives the PT.

The increase of the number of IR-active modes below T_c is not dramatic as one would expect in the case of a triclinic low-temperature phase, and it can be well explained by the lowering of the crystal symmetry just to the monoclinic phase without cell doubling. Several new modes in the FE phase, which are not seen in any other spectra in the PE phase, are probably slightly active already in the PE phase, but in consequence of their small strengths can be seen only at low temperatures, where all of the modes have much less damping.

The conclusion in [15] that the FE phase has triclinic symmetry is based on the experimental results of dielectric measurements, where the anomaly in the two components of the permittivity (ε'_a , ε'_b) was observed, and also polarization (P_a , P_b) parallel to the two crystallographic axes was found. Glushkov *et al* [15] suggested a two-dimensional OP from the Brillouin zone boundary [15]. However, this OP cannot simply explain the anomaly in ε'_a , ε'_b [13, 15], s_{44} and s_{55} [13] already seen above T_c . It can have an influence on these quantities only below T_c . The triclinic FE phase, however without doubling of the unit cell, can be theoretically obtained also in a different way by two one-dimensional OPs (of different symmetries) with the aid of a triggering mechanism [20]. Nevertheless, in this case the PT should be of first order in contradiction with the experimental results [13, 21], where the second-order PT is clearly seen.

To understand the anomalies in s_{44} [13] and ε'_a [13, 15] we note that they are two orders of magnitude smaller than those in s_{55} and ε'_b , respectively. This can be explained either by a small misalignment of the samples or by a partial softening of another transverse acoustic mode with the u_{bc} -deformation. The latter effect is already known from other materials, e.g. betaine fumarate and betaine borate both with ferroelastic PTs [22]. Also the spontaneous polarization P_a [15] is two orders of magnitude smaller than P_b ; therefore we suggest that misalignment is highly probable and the FE phase has monoclinic symmetry.

Our final remarks concern the microscopic origin of the PT and the dielectric dispersion. As suggested by Maeda and Ikeda [13] and confirmed by our FIR measurements, no polar soft phonon exists and the PT is of order–disorder type. The order parameter might be a non-polar collective reorientation of the NH_4 groups of B_2 symmetry. The characteristic frequencies of these reorientations in the PE phase must be much lower than the optic phonon range. In their thermodynamic theory, Maeda and Ikeda [13] neglected the direct bilinear coupling between these reorientations and optic phonon modes; however, they introduced a strong bilinear coupling of the order parameter with the transverse acoustic mode driven by the s_{55} -compliance. As this mode is also bilinearly coupled with the polar optic modes of B_2 symmetry through the piezoelectric effect, it becomes clear that some activation of the reorientational motion in the $\varepsilon'_b(\omega)$ dielectric spectrum is also to be expected, at least through the indirect bilinear coupling with the optic modes. Therefore, in addition to the piezoelectric resonances [13], the dielectric dispersion should reveal also a relaxational

process in a comparable or higher frequency range up to 2 MHz (above this frequency no dispersion was observed [10]). The corresponding characteristic relaxation frequency—not yet observed—plays the role of the critical relaxation for this PT. Therefore detailed dielectric dispersion data are highly desirable to quantify further the thermodynamic theory given by Maeda and Ikeda [13] and to shed light on the PT dynamics in LAT.

Finally we can conclude that our IR and Raman data are consistent with the equitranslation order–disorder PT from the orthorhombic to the monoclinic phase. The phase transition temperature is slightly sensitive to the hydrostatic pressure and its value decreases from 98 K at ambient pressure down to 91 K at 400 MPa.

Acknowledgments

The authors are grateful to V Dvořák and J Holakovský for valuable discussions. This work was supported by the Alexander von Humboldt Foundation and the Grant Agency of the Czech Republic (project No 202/95/1393).

References

- [1] Matthias B T and Hulm J K 1951 *Phys. Rev.* **82** 108
- [2] Merz W J 1951 *Phys. Rev.* **82** 562
- [3] Shirane G, Jona F and Pepinsky R 1955 *Proc. IRE* **43** 1776
- [4] Hinazumi H and Mitsui T 1972 *Acta Crystallogr. B* **28** 3299
- [5] Abe R and Matsuda M 1974 *J. Phys. Soc. Japan* **37** 437
- [6] Abe R and Matsuda M 1973 *J. Phys. Soc. Japan* **34** 686
- [7] Frazer B C 1962 *J. Phys. Soc. Japan Suppl. B-II* **17** 376
- [8] Maeda M, Suzuki I and Abe R 1975 *J. Phys. Soc. Japan* **38** 592
- [9] Maeda M, Suzuki I and Abe R 1975 *J. Phys. Soc. Japan* **39** 1319
- [10] Sawada A, Udagawa M and Nakamura T 1977 *Phys. Rev. Lett.* **39** 829
- [11] Udagawa M, Kohn K and Nakamura T 1978 *Ferroelectrics* **21** 329
- [12] Terauchi H, Takenaka H, Matsumori N and Sawada A 1978 *J. Phys. Soc. Japan* **44** 1751
- [13] Maeda M and Ikeda T 1977 *J. Phys. Soc. Japan* **42** 1931
- [14] Jain A K and Upreti G C 1981 *J. Chem. Phys.* **75** 1623
- [15] Glushkov V F, Magataev V K and Gladkii V V 1994 *Fiz. Tverd. Tela* **36** 1311 (Engl. Transl. 1994 *Phys. Solid State* **36** 716)
- [16] Bornarel J, Fousková A, Guyon P and Lajzerowicz J 1966 *Proc. Int. Mtg on Ferroelectricity (Prague)* vol II (Prague: Institute of Physics of the Czechoslovak Academy of Sciences) pp 81–90
- [17] Kamba S, Schaack G, Petzelt J and Březina B 1996 *J. Phys.: Condens. Matter* **8** 4631
- [18] Samara G A and Peercy P S 1981 *Solid State Physics, Advances in Research and Applications* vol 36, ed H Ehrenreich, F Seitz and D Turnbull (New York: Academic) p 1
- [19] Kamba S, Schaack G and Petzelt J 1995 *Phys. Rev. B* **51** 14998
- [20] Holakovský J 1973 *Phys. Status Solidi b* **56** 615
- [21] Makita Y and Wada K 1973 *J. Phys. Soc. Japan* **34** 1111
- [22] Unruh H-G 1995 *Phase Transitions* **55** 155